Eur. Phys. J. B (2014) 87: 167
DOI: 10.1140/epjb/e2014-50223-1

THE EUROPEAN PHYSICAL JOURNAL B

Regular Article

Persistent current of relativistic electrons on a Dirac ring in presence of impurities

Sumit Ghosh[1,a] and Arijit Saha[2,b]

[1] S.N. Bose National Centre for Basic Sciences, Salt Lake, 700098 Kolkata, India
[2] Department of Physics, University of Basel Klingelbergstrasse 82, 4056 Basel, Switzerland

Received 1st April 2014 / Received in final form 14 May 2014
Published online 1 August 2014 –

Abstract. We study the behaviour of persistent current of relativistic electrons on a one dimensional ring in presence of attractive/repulsive scattering potentials. In particular, we investigate the persistent current in accordance with the strength as well as the number of the scattering potential. We find that in presence of single scatterer the persistent current becomes smaller in magnitude than the scattering free scenario. This behaviour is similar to the non-relativistic case. Even for a very strong scattering potential, finite amount of persistent current remains for a relativistic ring. In presence of multiple scatterer we observe that the persistent current is maximum when the scatterers are placed uniformly compared to the current averaged over random configurations. However if we increase the number of scatterers, we find that the random averaged current increases with the number of scatterers. The latter behaviour is in contrast to the non-relativistic case.

1 Introduction

Persistent current (PC) in a normal metallic ring has drawn significant attention in the last few decades [1–11]. Due to the recent advancement in fabrication techniques, it has now become possible to observe this current experimentally [12–15] in normal metal rings. Such current is also observed in carbon nanotube rings [16–18] in which the low energy spectrum of electrons require a relativistic description. There is a large number of intriguing literatures on the energy levels and PC of relativistic fermions [19–21] involving the condensed matter systems like graphene [22–29] and topological insulator [30] in which the low energy spectrum is also described by Dirac Hamiltonian. For large particle mass the prediction of both relativistic and nonrelativistic theory is similar, but for small particle mass they differ significantly. Some remarkable difference can be observed in case of scattering and barrier penetration at this mass regime. Although the nature of PC is well-studied for the condensed matter systems, there are still several aspects of relativistic fermions which needs a further detailed analysis regarding scattering by a potential barrier/well on a ring geometry.

Motivated by the above mentioned facts, in this article we investigate the nature of energy and PC spectra of a relativistic fermion on a one dimensional (1-D) ring in presence of both attractive and repulsive scattering potentials. Here we consider finite width as well as different strengths and configurations for the scatterers along the ring. We adopt the relativistic Kronig-Penney model [31] to carry out our analysis which has been widely used in recent years for studying the effect of potential barriers in graphene [32–37]. Also the model we adopted here is sufficient to describe the low energy spectrum of a monolayer graphene with single valley and finite mass gap. Previously such model has been considered in reference [28] where they have considered quantum rings made out of single layer graphene described by the Dirac Hamiltonian with a finite mass term. Motivated by their model, in our work we consider Dirac Hamiltonian with a finite mass gap (similar to single valley of a monolayer graphene with a constant mass gap) and the effects of single and random impurities on energy spectrum and persistent current therein. We also assume that, in our model, impurities do not break the valley degeneracy such that considering single valley is a legitimate approximation.

Although the model is developed for relativistic particles, but for large particle mass it can predict the non-relativistic nature as well. Our main focus is to investigate the behaviour of PC with different configurations and strengths of the scatterers. We also investigate the variation of the maximum PC with single scattering potential and show how the rate of change of PC varies with respect to the strength of scattering potential for different mass gap. Finally we make a comparison among random configurations of multiple scattering potentials along the ring

[a] *Present address*: PSE Division, King Abdullah University of Science and Technology, Thuwal 23955-6900, Saudi Arabia.
[b] e-mail: arijit.saha@unibas.ch

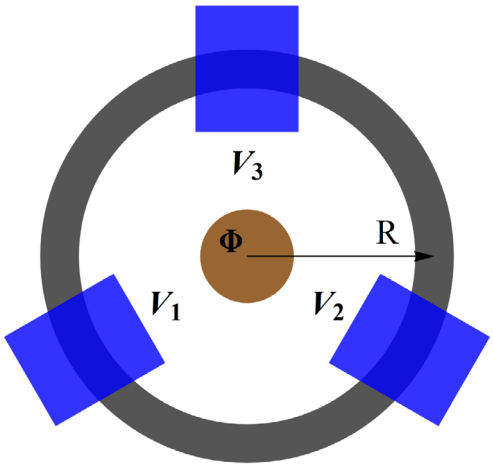

Fig. 1. Schematic of our geometry where a magnetic flux Φ is threaded through a ring of radius R with relativistic electrons. Here V_1, V_2 and V_3, etc. correspond to the scalar impurities modelled as potential wells/barriers placed along the ring.

and show that if the fraction of ring covered by the impurities remains the same, PC after the disorder average becomes larger in magnitude with the increase of number of impurities. The latter behaviour is in contrast to the non-relativistic case.

The organization of the rest of the article is as follows. In Section 2 we present a generic description of our model for the quantum ring with relativistic electrons in presence of scattering potentials. In Section 3 we analyse the spectrum and PC for a relativistic quantum ring in presence of single scatterer of different strenghts. In Section 4 we discuss the PC in presence of uniform as well as random configurations of scatterers after disorder average. Finally in Section 5, we present our summary and conclusion.

2 Model and method

A quantum ring presents an ideal realization of an infinite lattice with periodicity $2\pi R$, R being its radius. Due to this periodicity one can use the Kronig-Penney (KP) model [38] to study the effect of impurities in such a ring. In our analysis we incorporate the relativistic version of the KP model. This model was first introduced to study the behaviour of quarks in a periodic nuclear lattice [31]. Here we have generalized this approach for multiple scatterer in an unit cell. The method basically involves two steps – (i) finding the solution of Dirac equation in different regions of the ring and (ii) connecting the solutions using the transfer matrices. Here we model our impurities within the relativistic ring as rectangular well/barrier with finite width and strength. For vanishing scattering potential strength, our results match exactly with the analytical predictions [28].

Here we briefly discuss our model which starts with the Dirac equation for electrons on a 1-D quantum ring. The model Hamiltonian is sufficient to describe the low energy spectrum of a graphene monolayer for single valley with a

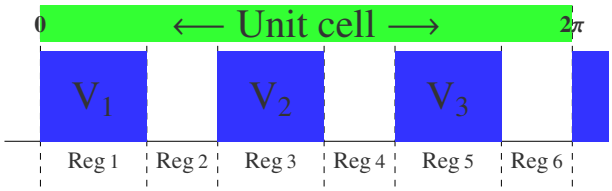

Fig. 2. Schematic of the unit cell in which the cell is divided into different regions and some regions are characterized by the scattering potentials V_1, V_2, V_3 chosen randomly along the cell.

constant mass gap [28]. The Dirac equation is given by:

$$\begin{pmatrix} \delta & -i\frac{\hbar c}{R}e^{-i\varphi}\left(-\frac{1}{2}-i\frac{\partial}{\partial\varphi}\right) \\ -i\frac{\hbar c}{R}e^{i\varphi}\left(-\frac{1}{2}+i\frac{\partial}{\partial\varphi}\right) & -\delta \end{pmatrix}\begin{pmatrix}\zeta_1\\ \zeta_2\end{pmatrix} = E\begin{pmatrix}\zeta_1\\ \zeta_2\end{pmatrix}, \quad (1)$$

where R is the radius of the ring and ζ_1 and ζ_2 are scalar functions of the angular variable φ satisfying the normalization condition $|\zeta_1|^2 + |\zeta_2|^2 = 1$. Here δ corresponds the mass term or the band gap in case of condensed matter system. The Dirac equation within the square well/barrier can be obtained by replacing the energy E with $E - V_0$, where V_0 is the strength of the well/barrier. Hence we obtain two sets of linearly independent solutions characterized by a spatial part $e^{il_+\varphi}$ and $e^{il_-\varphi}$ which can be written as

$$\psi_l^{\pm}(\varphi) = \begin{pmatrix}\zeta_1^{\pm}\\ \zeta_2^{\pm}\end{pmatrix} = \begin{pmatrix}1\\ i\kappa_{\pm}e^{i\varphi}\end{pmatrix}e^{il_{\pm}\varphi}, \quad (2)$$

where $\kappa_{\pm} = \frac{\hbar c}{R}\frac{1/2+l_{\pm}}{E+\delta}$.

Now we divide the ring into different regions in space (see Fig. 2) and define matrix $\Omega_n(\varphi) = (\Psi_n^1(\varphi), \Psi_n^2(\varphi))^T = C_n W_n(\varphi)$ for the nth region[1], where

$$\Psi_n^{1,2}(\varphi) = A_n^{1,2}\psi_l^+(\varphi) + B_n^{1,2}\psi_l^-(\varphi), \quad (3)$$

$$C_n = \begin{pmatrix}A_n^1 & B_n^1\\ A_n^2 & B_n^2\end{pmatrix}; \qquad W_n(\varphi) = \begin{pmatrix}\zeta_1^+ & \zeta_2^+\\ \zeta_1^- & \zeta_2^-\end{pmatrix}. \quad (4)$$

Hence solution for any individual region can be characterised by the corresponding coefficient matrix C_n. For two consecutive regions, C_n will be connected by a suitable transfer matrix such that $C_{n+1} = T_n C_n$ [31]. By applying this transfer matrix method sequentially in every region of the ring one can find T_n for every region in terms of the corresponding $W_n(\varphi)$ from the continuity of $\Omega_n(\varphi)$. Now, if a ring has N number of such distinct regions in space, then the transfer matrix for the entire ring can be defined as $C_{N+1} = T_R C_1$, where $T_R = T_N T_{N-1} \ldots T_1$. Combining the latter with the periodic boundary condition $\Psi_l^{1,2}(2\pi) = e^{\pm i2\pi\Phi/\Phi_0}\Psi_l^{1,2}(0)$ [3] we finally obtain our energy band equation as

$$2\cos(2\pi\Phi/\Phi_0) = \mathrm{Tr}\,[T_R], \quad (5)$$

[1] Here we have omitted the index l for $\Psi_n(\varphi)$, $\Omega_n(\varphi)$ and $W_n(\varphi)$.

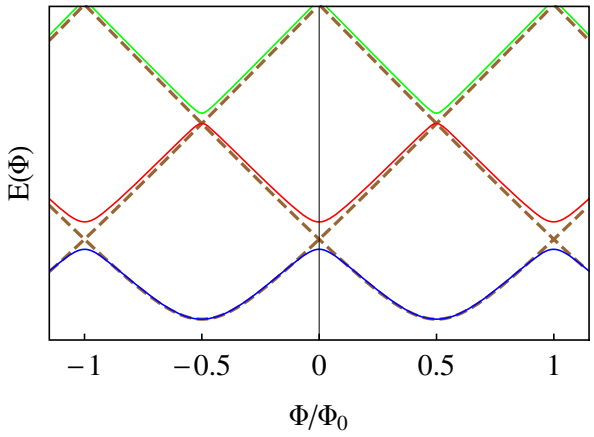

Fig. 3. Energy spectrum for the relativistic particle with $\delta = 14$ meV as a function of the flux without (dashed line) as well as with (solid line) single scattering potential of strength $V_0 = 35$ meV. The radius of the Dirac ring is chosen to be $R = 10$ nm.

where in equation (5) the role of the Bloch vector is played by the magnetic flux. Hence, the PC can be obtained from the band structure according to the well-known formula [3,4]

$$I_P = -c\frac{\partial E(\Phi)}{\partial \Phi}. \quad (6)$$

The same model can be easily modified for a one dimensional ring made of monolayer graphene by replacing the velocity of light (c) with the Fermi velocity ($v_F \sim 10^6$ m/s) [28]. In the following sections we will use v_F which would be helpful to obtain a quantitative estimation of the PC for condensed matter systems.

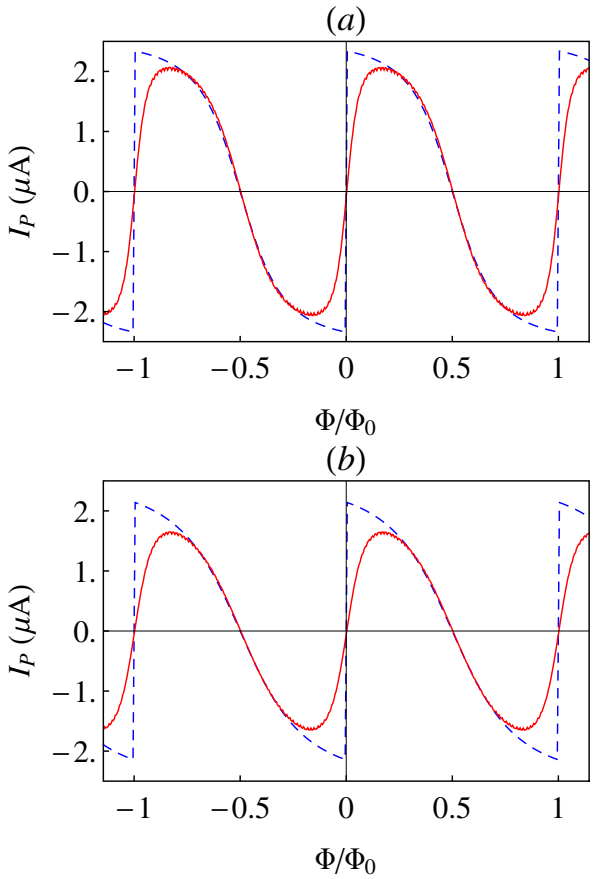

Fig. 4. Variation of PC as a function of the flux for massive relativistic electrons is shown for (a) $\delta = 14$ meV and (b) $\delta = 21$ meV without (blue dashed line) and with (red solid line) scattering potential $V_0 = 35$ meV. The radius of the Dirac ring is chosen to be $R = 10$ nm.

3 Single scattering potential

In this section we discuss the energy spectrum and the PC for massive relativistic Dirac electrons on a ring in presence of single scattering potential with various height and width.

3.1 Effect of mass gap and height

Even in absence of any scatterer the energy spectrum of a relativistic Dirac particle is not simply a quadratic function of the flux Φ [28]. For large mass the dependence appears to be approximately quadratic (see Fig. 3) and its change due to the addition of a single scatterer is similar to the nonrelativistic case [3,4]. Here we have chosen positive scattering potential ($V_0 > 0$) for our analysis. Similar behaviour can be observed for a negative scattering potential ($V_0 < 0$) which will be discussed later.

In presence of a single scatterer a gap opens up in the spectrum (see Fig. 3) due to which the magnitude of the maximum PC is reduced (see solid line of Figs. 4a and 4b) than the scattering free case (dashed line of Figs. 4a and 4b). Such behaviour is similar to the nonrelativistic situation where the maximum value of the PC always becomes smaller in magnitude in presence of single scatterer of equal strength [3,4].

In Figures 4a and 4b we show the PC for two different mass gaps. One can see that the amplitude of the PC decreases with the increase of the mass term δ. From this two figures, the amplitude of maximum current is decreasing linearly with the particle mass. Keeping in mind that PC is also inversely proportional to the square of the ring radius [19,20], we see that for a ring with radius 300 nm if we substitute the particle mass by electron mass, i.e. $\delta = 500$ eV, we can roughly estimate that the current will be of the order of 0.1 nA, which is in fair agreement with the experimental finding [15]. One can also see that the Φ_0 periodicity is still there in the relativistic case with the characteristic shift of $\Phi_0/2$ [19,20].

In Figures 5a and 5b we show the behaviour of the PC in presence of single potential barrier with different strengths. It is clear that the magnitude of the PC becomes smaller and smaller as we increase the strength of the potential which is quite expected. However what distinguish it from nonrelativistic situation is that if we keep increasing the strength of the scatterer, the maximum current

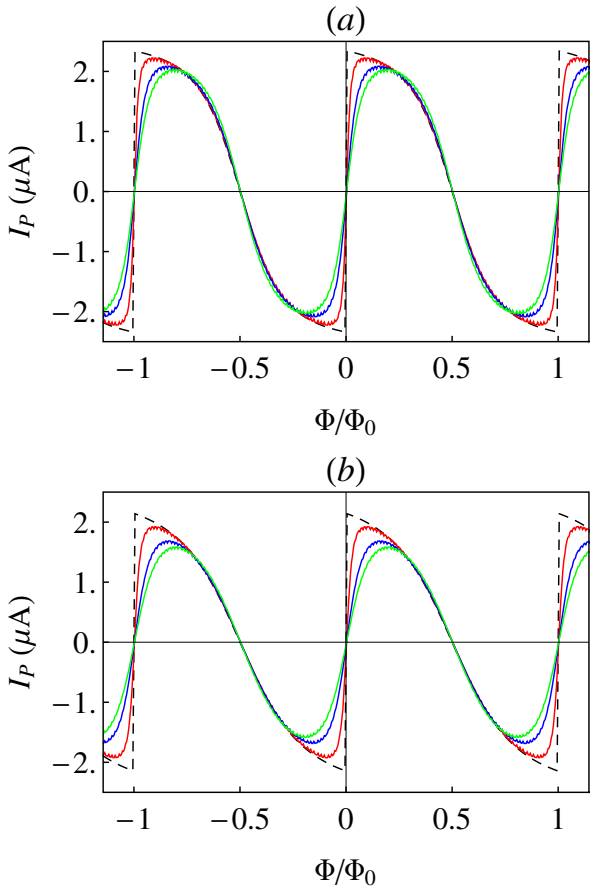

Fig. 5. Variation of PC as a function of the flux in presence of single scattering potential with different strengths for (a) $\delta = 14$ meV and (b) $\delta = 21$ meV. Here different lines correspond to the attractive scattering potentials with $V_0 = 10$ meV (red), $V_0 = 30$ meV (blue) and $V_0 = 50$ meV (green), respectively. The black dashed line depicts the scattering free PC. The radius of the ring is $R = 10$ nm.

instead of reaching zero, reaches a finite saturation value. We shall discuss about this case in the next section.

3.2 Variation of maximum current

In this section we present a comparative analysis between the effect of the attractive and repulsive single scattering potential on PC for the relativistic case (see Fig. 6).

The variation of maximum current is almost symmetric around $V_0 = 0$. The asymmetry is an outcome of the fact that we have considered only positive energy particles. One can see that as we consider smaller values of mass term (δ) the behaviour of PC becomes more and more symmetric. Note that in both cases the maximum magnitude of the PC decreases as we increase the strength (V_0) of the potential. The relativistic PC remains at a finite value even in the presence of strong scattering potential. This is due to Klein tunneling [39] which allows electrons to pass through the barrier although the particle energy is less than the barrier height when the barrier height exceed twice the particle rest mass energy. Also note that, for

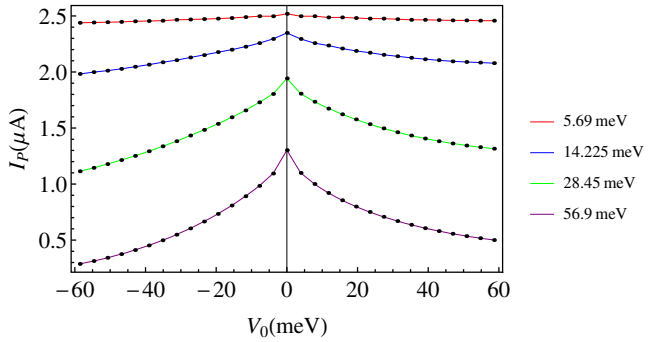

Fig. 6. Variation of maximum PC is shown with respect to the strength of a single scattering potential for relativistic electrons with four different mass gaps δ (written in legend). The radius of the ring is chosen to be $R = 10$ nm.

$\delta \to 0$, PC remains almost constant, which is in complete agreement with the fact that massless particles cannot be affected by potential barriers.

The behaviour of maximum PC depicted in Figure 6 can be further illustrated by the phenomena of Klein tunneling for the relativistic case. In presence of single impurity, if the scattering potential strength $V_0 \to \infty$ and the mass term $\delta \to 0$, then the barrier becomes transparent (transmission probability through the barrier $T \sim 1$) to the incident electrons due to Klein tunneling. In this case we obtain large and almost constant PC as shown in Figure 6.

On the other hand, if both V_0 and δ are large but finite, then transmission through the barrier becomes $0 < T < 1$ as shown in reference [39] and we obtain the maximum value of PC which is smaller in magnitude compared to the previous case mentioned earlier. Hence, if we increase δ further (keeping V_0 same as before), then T becomes smaller in magnitude than before and the corresponding PC is further reduced. The latter behaviour is also depicted in Figure 6.

4 Multiple impurities

Here we discuss the behaviour of PC for the Dirac fermions in presence of multiple scattering potentials with uniform as well as random configurations (quenched disorder). In the latter case, we assign the scattering potentials randomly on the ring for a particular configuration and consider the average of energy/current over a large (∼1000) number of configurations which is more realistic as far as the experimental situation is concerned. The corresponding mean free path (ξ) is of the order of typical system size (L) i.e. $\xi \sim L$ as in our model we considerelastic scatterers which do not break the phase coherence of electrons.

4.1 Uniform configuration

Here we study a relativistic ring with scattering potentials covering 40% of the ring for uniform spacing. In particular

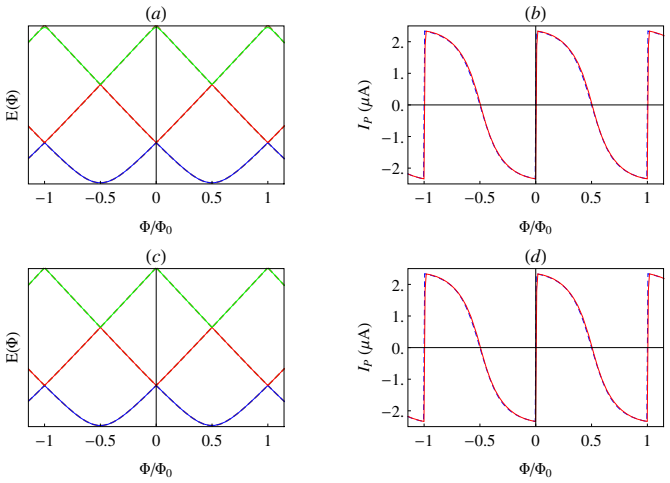

Fig. 7. The energy spectrum of the quantum ring for the relativistic case is shown in (a) and (c) with uniformly spaced 3 and 10 scattering potentials, respectively such that they cover 40% size of the ring. The brown dashed line corresponds to the scattering free ring. Variation of PC is shown in (b) and (d). In all these cases, the average strength of the scattering potentials are chosen to be $V_0 = 35$ meV. The value of the other parameters are $\delta = 14$ meV and $R = 10$ nm.

here we discuss the results with 3 and 10 impurities. The uniform configuration almost overlap with the scattering free spectrum as shown in Figures 7a and 7c. Also the magnitude of the corresponding PC remains almost the same as the scattering free case which is shown in Figures 7b and 7d. The reason behind such behaviour can be the resonance scattering inside the ring aided by the relativistic tunnelling in presence of uniform configuration of impurities.

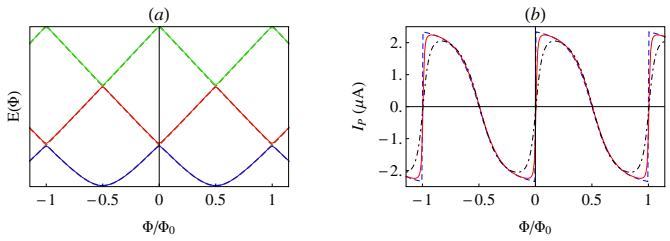

Fig. 8. Disorder averaged energy (a) and PC (b) spectra for 3 scatterer which cover 40% size of the ring. The brown dashed line in (a) corresponds to the scattering free ring. The solid red line in (b) is the disorder averaged current and the blue dashed line is the scattering free case. The single scatterer PC is shown by the black dot-dashed line which is less than the 3 scatterer PC. In all these cases, the average strength of the scattering potentials are chosen to be $V_0 = 35$ meV. The value of the other parameters are $\delta = 14$ meV and $R = 10$ nm.

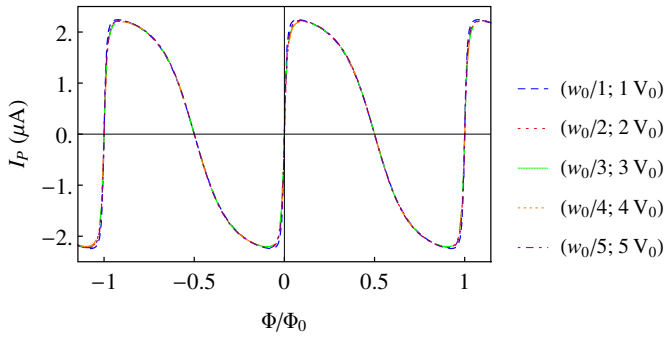

Fig. 9. Disorder averaged PC for three scatterer configurations with different width and height of impurities such that their product remains the same. Individual widths and heights are written in legend. Other parameter values are $w_0 = 40\%$ (total percentage of ring covered by scattering potential), $\delta = 14$ meV, $R = 10$ nm and $V_0 = 35$ meV.

4.2 Random configuration: disorder average

In this subsection we consider multiple impurities and study the PC averaged over different random configurations. For better contrast with the scattering free and single scatterer case, first we consider 3 scatterers along the ring. The PC becomes larger in magnitude than the single scatterer case, but remains less than the scattering free scenario. The corresponding behaviour of disorder averaged spectrum and PC in presence of random scattering configurations is shown in Figures 8a and 8b, respectively.

Note that in our analysis we have used a finite width for our scatterer. However it can be easily generalised for a δ-function potential by considering the zero width limit. Reduction of the width of the scatterer will produce the same effect as reducing the potential strength. If we approach to the zero width limit in such a way that the product of the scattering width and strength remain the same, the resulting PC will also exhibit the similar behaviour (see Fig. 9).

In Figures 10a and 10b we show the disorder averaged PC in presence of attractive and repulsive randomly spaced scattering configurations, respectively. The behaviour of PC is similar for the two cases. Note that the disorder averaged PC is enhanced is magnitude than the single scatterer case as we increase the number of random configurations. This behaviour is in contrast to the non-relativistic case where PC becomes smaller in magnitude than the single scatterer case due to the electron localization in presence of random impurities [3,4].

In presence of a scattering potential the transmissivity of a particle decreases causing a decrease in current. However for relativistic particle, due to Klein tunnelling, there can be a resonant transmission at an energy less than the barrier height. In presence of multiple scatterers, the number of resonant energy levels also increases which can cause an increase in the current under appropriate condition. Qualitatively, due to the presence of multiple scatterers there can be resonant tunneling through the scattering potentials in contrast to the single impurity.

Resonant tunneling has been studied in case of double barriers/wells in graphene in reference [40], considering a similar simplified model like us in case of graphene with a constant mass gap. Hence, some random configurations

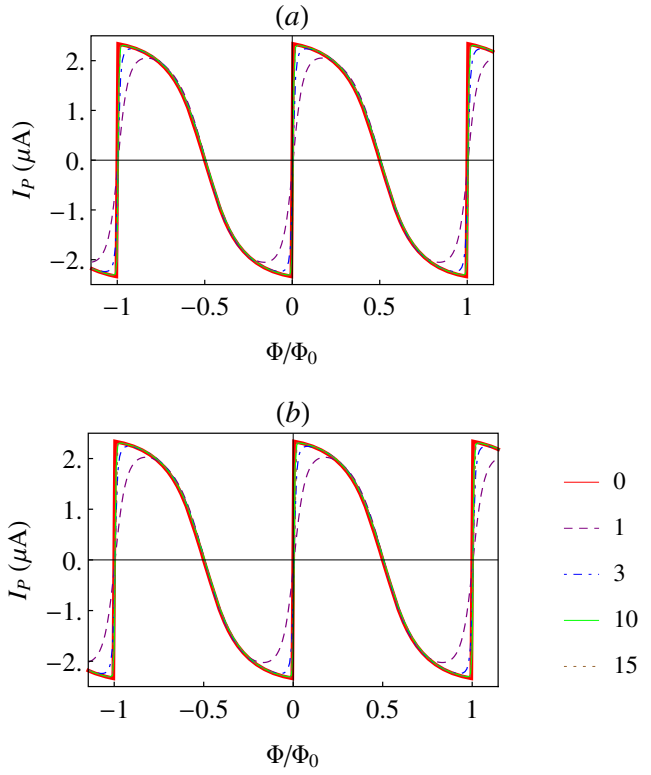

Fig. 10. Disorder averaged PC for different number of scatterer configurations covering 40% of total ring with (a) positive and (b) negative potential for $\delta = 14$ meV, $R = 10$ nm and $V_0 = \pm 35$ meV.

of scattering potentials can give rise to resonant tunneling through them which is the reason for the enhancement of PC in the relativistic case. On the other hand, in the non-relativistic case, random scatterers always cause the electron wave function to be localized at the scattering centres (Anderson localization) due to which PC becomes smaller in magnitude as shown in references [3,4].

5 Summary and conclusion

To summarize, in this article we have presented the PC for massive relativistic electrons on a 1-D Dirac ring in presence of single as well as multiple attractive and repulsive scattering potentials. In presence of single scattering potential, the maximum PC for the Dirac ring decreases with the strength of the scatterer with a rate inversely proportional to the particle mass. Even in presence of strong potential, a finite value of the PC remains for a massive particle. These two outcomes can be identified as a manifestation of Klein tunnelling. Finally in presence of multiple scattering potentials with both uniform and random configurations the PC is increased in magnitude than that of the single scatterer case after the disorder average due to resonant tunneling. This behaviour is in contrast to the non-relativistic case where PC becomes smaller in magnitude than the single scatterer case in presence of random scattering potentials.

In presence of multiple subbands (many electrons) for a ring with finite width, our results for the PC remain qualitatively the same as long as the subbands are not interacting to each other. Although, if one considers band mixing, then the qualitative feature of the PC remains to be the same apart from the quantitative change in the current. Moreover, the period of PC always remains to be 2π.

The Dirac Hamiltonian we considered here is quite suitable for a monolayer graphene ring considering single valley [28]. As far as the practical numbers are concerned, according to our numerical analysis, for a typical band gap of $\delta \approx 14$ meV [41] and impuity strength $V_0 \approx 35$ meV, a PC of magnitude $I_P \approx 2$ μA can be obtained for a Dirac ring of radius $R = 10$ nm which can be measured experimentally.

S.G. likes to acknowledge the financial support by the CSIR, India. The work of A.S. has been supported by the Swiss NSF, NCCR Nanoscience, and NCCR QSIT.

References

1. M. Büttiker, Y. Imry, R. Landauer, Phys. Lett. A **96**, 365 (1983)
2. R. Landauer, M. Büttiker, Phys. Rev. Lett. **54**, 2049 (1985)
3. H.F. Cheung, Y. Gefen, E.K. Riedel, W.H. Shih, Phys. Rev. B **37**, 6050 (1988)
4. H.F. Cheung, E.K. Riedel, Y. Gefen, Phys. Rev. Lett. **62**, 587 (1989)
5. A. Altland, S. Iida, A. Müeller-Groeling, H.A. Weidenmüller, Ann. Phys. **219**, 148 (1992)
6. A. Altland, S. Iida, A. Müeller-Groeling, H.A. Weidenmüller, Europhys. Lett. **20**, 155 (1992)
7. J.F. Weisz, R. Kishore, F.V. Kusmartsev, Phys. Rev. B **49**, 8126 (1994)
8. W. Rabaud, L. Saminadayar, D. Mailly, K. Hasselbach, A. Benoit, B. Etienne, Phys. Rev. Lett. **86**, 3124 (2001)
9. M. Moskalets, M. Büttiker, Phys. Rev. B **66**, 245321 (2002)
10. J. Splettstoesser, M. Governale, U. Zülicke, Phys. Rev. B **68**, 165341 (2003)
11. I.O. Kulik, Low Temp. Phys. **36**, 841 (2010)
12. L.P. Levy, G. Dolan, J. Dunsmuir, H. Bouchiat, Phys. Rev. Lett. **64**, 2074 (1990)
13. D. Mailly, C. Chapelier, A. Benoit, Phys. Rev. Lett. **70**, 2020 (1993)
14. N.A.J.M. Kleemans et al., Phys. Rev. Lett. **99**, 146808 (2007)
15. A.C. Bleszynski-Jayich et al., Science **326**, 272 (2009)
16. M. Szopa, M. Margańska, E. Zipper, Phys. Lett. A **299**, 593 (2002)
17. S. Latil, S. Roche, A. Rubio, Phys. Rev. B **67**, 165420 (2003)
18. R.B. Chena, B.J. Lub, C.C. Tsaib, C.P. Changc, F.L. Shyud, M.F. Lin, Carbon **42**, 2873 (2004)
19. I.I. Cotaescu, E. Papp, J. Phys.: Condens. Matter **19**, 242206 (2007)
20. S. Ghosh, Adv. Condens. Mater. Phys. **2013**, 592402 (2013)

21. D. Sticlet, B. Dora, J. Cayssol, Phys. Rev. B **88**, 205401 (2013)
22. K. Ino, Phys. Rev. Lett. **81**, 1078 (1998)
23. K. Ino, Phys. Rev. Lett. **81**, 5908 (1998)
24. K. Ino, Phys. Rev. B **62**, 6936 (2000)
25. A.H. Castro Neto, F. Guinea, N.M.R. Peres, Phys. Rev. B **73**, 205408 (2006)
26. P. Recher, B. Trauzettel, A. Rycerz, Ya.M. Blanter, C.W.J. Beenakker, A.F. Morpurgo, Phys. Rev. B **76**, 235404 (2007)
27. M. Zarenia, J.M. Pereira Jr., F.M. Peeters, G.A. Farias, Nano Lett. **9**, 4088 (2009)
28. M. Zarenia, J.M. Pereira, A. Chaves, F.M. Peeters, G.A. Farias, Phys. Rev. B **81**, 045431 (2010)
29. B.-L. Huang, M.-C. Chang, C.-Y. Mou, J. Phys.: Condens. Matter **24**, 245304 (2012)
30. P. Michetti, P. Recher, Phys. Rev. B **83**, 125420 (2011)
31. B.H.J. McKellar, G.J. Stephenson Jr., Phys. Rev. C **35**, 2262 (1987)
32. M. Barbier, F.M. Peeters, P. Vasilopoulos, J. Milton Pereira Jr., Phys. Rev. B **77**, 115446 (2008)
33. M. Barbier, P. Vasilopoulos, F.M. Peeters, Phys. Rev. B **80**, 205415 (2009)
34. M. Barbier, P. Vasilopoulos, F.M. Peeters, Phys. Rev. B **82**, 235408 (2010)
35. M.R. Masir, P. Vasilopoulos, F.M. Peeters, J. Phys.: Condens. Matter **22**, 465302 (2010)
36. S. Gattenlöhner, W. Belzig, M. Titov, Phys. Rev. B **82**, 155417 (2010)
37. A. Matulis, M.R. Masir, F.M. Peeters, Phys. Rev. A **86**, 022101 (2012)
38. C. Kittel, *Introduction to Solid State Physics* (John Wiley & Sons, 2004)
39. M.R. Setare, D. Jahani, Physica B **405**, 1433 (2010)
40. J.M. Pereira Jr., P. Vasilopoulos, F.M. Peeters, Appl. Phys. Lett. **90**, 132122 (2007)
41. Lijie Ci et al., Nat. Mater. **9**, 430 (2010)